The Monte Carlo Method: Versatility Unbounded in a Dynamic Computing World
Chattanooga, Tennessee, April 17-21, 2005, on CD-ROM, American Nuclear Society, LaGrange Park, IL (2005)

AN EFFECTIVE CHARGE SCALING MODEL FOR IONIZATION OF PARTIALLY DRESSED HELIUM IONS WITH LIQUID WATER

Michael Dingfelder and Larry H. Toburen
Department of Physics
East Carolina University
Howell Science Complex, Greenville, NC 27858, USA
dingfelderm@mail.ecu.edu; toburenl@mail.ecu.edu

Herwig G. Paretzke
Institute of Radiation Protection
GSF - National Research Center for Health and Environment
Ingolstädter Landstraße 1, D-85764 Neuherberg, Germany
paretzke@gsf.de

ABSTRACT

Ionization cross sections for all charge states of the helium ion are calculated using an effective charge scaling approach. Within the plane wave Born approximation the ionization cross section for (dressed) ion impact can be related to a product of an effective charge and the ionization cross sections for proton impact. Different models for calculating effective charges for dressed ions are presented and discussed. Total ionization cross sections for helium ion impact on liquid water are calculated. Total stopping cross sections for alpha particle impact on liquid water are used as a benchmark criterion to evaluate the effective charge models. A model that reproduces ICRU recommended values for the stopping cross sections is adopted. Charge changing cross sections and the charge state approach to calculate stopping cross sections are briefly reviewed.

Key Words: heavy ion transport, cross sections, dressed ions.

1 INTRODUCTION

Track structure calculations of charged particles are useful for the understanding of early physical and chemical stages of radiation actions on matter in general. This holds true especially in radiation biology where a precise description of the spatial pattern of energy deposition by ionizing radiation is important for interpretation of results of mechanistic models. Track structure analysis based on Monte Carlo computer simulations uses the classical trajectory picture and follows the incident particle, as well as all secondary particles, from starting or ejection energies down to total stopping, by processing elastic and inelastic scattering events. Therefore, this kind of simulation requires reliable interaction cross sections of charged particles with atoms and molecules in matter under consideration for a wide energy range, from relativistic energies to total stopping. Liquid water, which is the dominant component in the biological cell of soft tissue, is used as a model substance for organic matter.

As fast helium ions pass through matter they interact elastically and inelastically with the target atoms or molecules under consideration. In this study, elastic scattering is neglected. Fast charged particles mainly excite and ionize target atoms or molecules, secondary electrons are ejected and the projectile remains in its charge state. When the alpha particle slows, electron capture and loss by the moving ion becomes increasingly important. In these processes the projectile changes its charge state by picking up or loosing some electrons. Different charge states of the ion will have different excitation and ionization probabilities due to the partial screening of the nuclear charge by projectile electrons. Simultaneous electron capture or loss by the projectile and excitation and/or ionization of the target, as well as of the projectile can also occur.

Detailed Monte Carlo simulation of alpha particle tracks requires knowledge of total and energy differential cross sections for excitation and ionization by He^{2+}, He^{+} and He^{0} as well as secondary electron emission spectra for all these charge states, and charge changing cross sections for one and two electron capture and loss.

In this work we focus on ionization cross sections for the different helium charge states, incident on liquid water. In the following we review and present different models for effective charge scaling and explore their influence on stopping cross sections.

2 IONIZATION FOR BARE IONS

Excitation and ionization cross sections for fast bare (fully ionized) projectiles (mass M and charge $Z_0 e$) are commonly described within the relativistic plane-wave Born approximation (PWBA) [1]. In this theory, the double differential cross section (DCS) $\mathrm{d}^2\sigma/\mathrm{d}E\mathrm{d}\Omega$ consists of a purely kinematical factor and the generalized oscillator strength (GOS) $\mathrm{d}f(Q,E)/\mathrm{d}E$, which fully characterizes the inelastic response of the target atom or molecule (atomic number Z_1). In detail, the DCS per target electron is given by [2]

$$\frac{\mathrm{d}^2\sigma_{\mathrm{ion}}}{\mathrm{d}E\mathrm{d}Q} = \frac{2\pi Z_0^2 e^4}{\mathrm{m_e} v_i^2}\frac{1}{E}\left(\frac{1}{Q(1+Q/2\mathrm{m_e}c^2)} + \frac{\beta_\mathrm{t}^2 E^2/2\mathrm{m_e}c^2}{[Q(1+Q/2\mathrm{m_e}c^2) - E^2/2\mathrm{m_e}c^2]^2}\right)\frac{\mathrm{d}f(Q,E)}{\mathrm{d}E}\,, \quad (1)$$

where E is the energy transfered, Q the recoil energy related to the momentum transfer q by $Q(Q+2\mathrm{m_e}c^2) = (cq)^2$, $\mathrm{m_e}c^2$ the electron rest energy, v_i the projectile incident velocity and β_t a kinematical factor given by

$$\beta_t^2 = \beta^2 - \frac{E^2}{Q(Q+2\mathrm{m_e}c^2)}\left(1 + \frac{Q(Q+2\mathrm{m_e}c^2) - E^2}{2E(\tau + Mc^2)}\right)^2. \quad (2)$$

Here, $\beta = v_i/c$ and τ is the total energy of the projectile.

The GOS is independent of the projectile and fully describes the electronic properties of the target material. It can either be calculated from microscopic theories [2] (target is single atom/molecule) or modeled semiempirically. The GOS can also be directly related to the dielectric response function $\varepsilon(Q,E)$ (DF) by

$$\frac{\mathrm{d}f(Q,E)}{\mathrm{d}E} = E\left(1 + \frac{Q}{\mathrm{m_e}c^2}\right)\frac{2Z_1}{\pi E_\mathrm{p}^2}\,\mathrm{Im}\left(\frac{-1}{\varepsilon(Q,E)}\right), \quad (3)$$

where E_p is the plasma energy of a homogeneous free-electron gas with electron density n, and $E_p^2 = 4\pi\hbar^2 n e^2/\mathrm{m_e}$. In case of liquid water, the dielectric response function has been modeled based on both, experimental information and theoretical constraints [3], and has been used to calculate excitation and ionization cross sections for electron [3] and proton [4] impact.

It can be shown that the DCS obtained from the dielectric formulation generalizes the quantum result for atoms and molecules [5]. In the case of a low-density medium both theories yield the same DCS. However, the dielectric formulation also considers medium polarization effects, known as Fermi density correction, which do not exist in low-density or gaseous targets.

3 IONIZATION FOR DRESSED IONS

When the heavy charged particle slows down, electron capture and loss processes become more and more important. These processes also change the charge state of the projectile. "Dressed" ions show different ionization and excitation cross sections than "bare" ions, also, simultaneous excitation and/or ionization of target and projectile can appear.

DCS for different bare ions scale with the nuclear charge Z_0^2 of the projectile and with the velocity v_i within the PWBA, as seen from Eq. (1). Therefore, within the PWBA the DCS for an alpha particle with a velocity v_i equals four times ($Z_0 = 2$) the DCS for a proton at the same velocity v_i. In the case of dressed ions the projectile electrons will screen the nuclear charge. In this case proton DCS will scale with an effective charge, which depends on the energy and/or the momentum transferred in the collision. The DCS for "dressed" or "bare" ion impact can be written as

$$\frac{\mathrm{d}\sigma_{\mathrm{ion}}}{\mathrm{d}E}(v_i) \;=\; Z_{\mathrm{eff}}^2(E)\,\frac{\mathrm{d}\sigma_{\mathrm{proton}}}{\mathrm{d}E}(v_i), \tag{4}$$

where Z_{eff} is the "effective charge" of the incident ion. For "bare" ions $Z_{\mathrm{eff}} = Z_0$. In the following section we will present and review different models for the effective charge and investigate their influence on total ionization and stopping cross sections for helium impact on liquid water.

At this point it should be mentioned that the PWBA is valid only for sufficient high incident particle energies, in the case of protons this is above approximately 300 keV. At lower energies, i. e., outside the validity of the PWBA, correction factors or semiempirical models are normally used. In the case of proton impact on liquid water we used a semiempirical model for the single (energy) differential cross sections based on works from Rudd and co-workers [6] as described in [4]. This model based on fits to experimental data contains non-PWBA corrections adequate for proton impact. A pure Z_0^2 scaling of these cross sections might overestimate these non-PWBA corrections for heavier bare ions, as indicated by Rudd et al. in Fig. 6 of Ref. [7]. On the other hand, effective charge Z_{ion} models for dressed ions might already contain these corrections.

4 EFFECTIVE CHARGE

The use of an effective charge accounts for screening of the nuclear charge by electrons bound to the incident ion that weaken the interaction potential. The effective charge depends strongly on the collisional energy transfer. Bound electrons provide effective screening of the nuclear charge of the projectile in collisions involving small energy transfers, whereas for large energy transfer screening is negligible. In the following we present two models from the literature and finally adopt a model of our own.

The model introduced by Toburen et al. [8] makes use of the correlation between the energy transfer E and the adiabatic interaction radius R_{ad} provided by the Massey criterion (all quantities in atomic units),

$$R_{\mathrm{ad}} \;=\; \frac{v_i}{E}, \tag{5}$$

where v_i is the incident ion velocity. This application of the Massey criterion clearly illustrates that small energy transfers correspond to interactions at large internuclear distances where bound electrons provide effective screening, whereas large energy transfers occur when the projectile deeply penetrates the target atom and screening by the projectile electrons is less important.

The effective nuclear charge of the incident ion in this model is given by

$$Z_{\mathrm{eff}} \;=\; Z - S(R), \quad \text{with} \quad S(R) \;=\; \sum_i N_i \int_0^R |\psi_i(r)|^2 r^2 \mathrm{d}r, \tag{6}$$

where $S(R)$ is the screening of the nuclear charge Z when viewed at a distance R from the nucleus, $\psi_i(r)$ is the normalized radial wave function for the ith bound electron, and N_i is the number of electrons in the ith subshell.

$S(R)$ can be calculated analytically using hydrogenic wave functions. The screening function for an electron in the $1s$, $2s$, or $2p$ atomic subshell is given by

$$S(R)_{1s} \;=\; 1 - \exp(-2\hat{R})(1 + 2\hat{R} + 2\hat{R}^2) \tag{7}$$

$$S(R)_{2s} \;=\; 1 - \exp(-2\hat{R})(1 + 2\hat{R} + 2\hat{R}^2 + 2\hat{R}^4) \tag{8}$$

$$S(R)_{2p} \;=\; 1 - \exp(-2\hat{R})(1 + 2\hat{R} + 2\hat{R}^2 + (4/3)\hat{R}^3 + (2/3)\hat{R}^4) \tag{9}$$

where $\hat{R}$ is the scaled adiabatic interaction radius given by $\hat{R} = (2t_{\mathrm{elec}}/E)(Q_{\mathrm{eff}}/n_{\mathrm{shell}})$; t_{elec} is the energy of an electron with the same velocity than the incoming ion and Q_{eff} is Slater's effective charge experienced by an electron bound in the nth subshell of the ion under consideration. [9].

The left panel of Fig. 1 shows the calculated total ionization (ion; upper curves) and excitation (exc; lower curves) cross sections σ_{ii} for the different charge states ($i = 0, 1, 2$) of helium on liquid water. A value of Q_{eff} = 1.7 is used for the $1s$ shell. Furthermore, a projectile-electron – target-electron interaction is added for each projectile electron (the

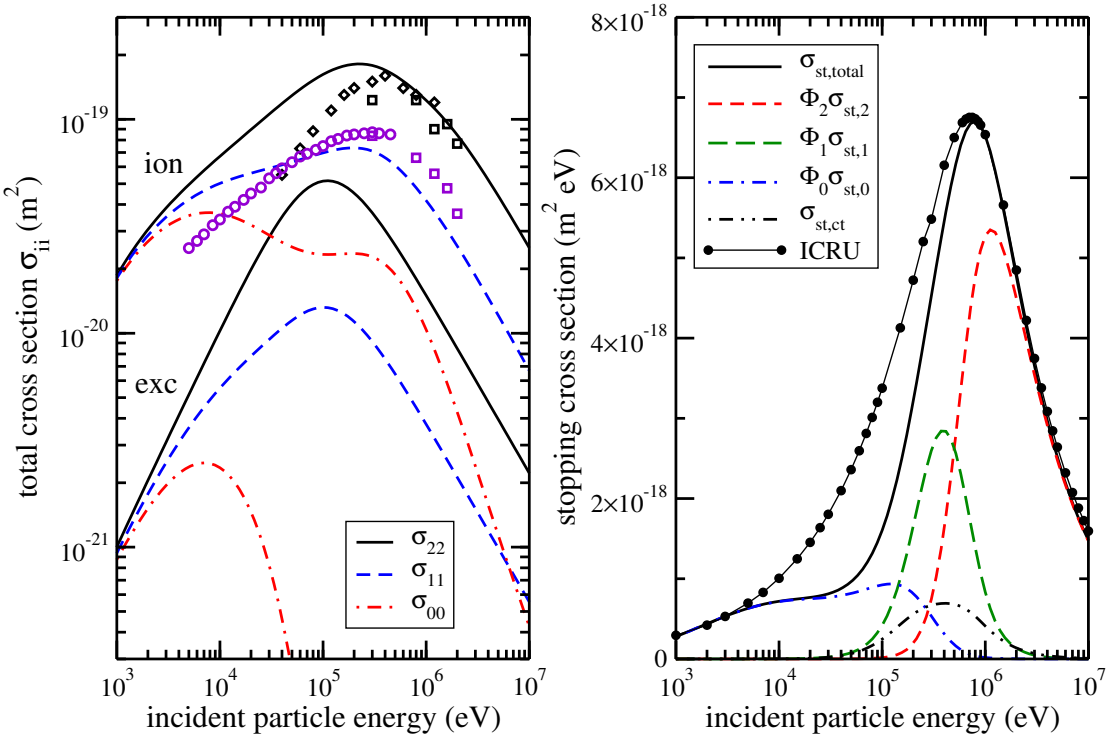

Figure 1: Ionization and stopping cross sections for helium impact on liquid water using the effective charge model of Toburen et al. [8]. The left panel shows total ionization (ion) and excitation (exc) cross sections for the different charge states ($i = 0, 1, 2$) together with experimental data for ionization taken from Refs. [7] (diamonds), [10] (circles), and [11] (squares). The right panel illustrates contributions to the total stopping cross sections from the different charge states ($\Phi_i\sigma_{\mathrm{st},i}, i = 0, 1, 2$) and charge changing processes ($\sigma_{\mathrm{st,ct}}$). The ICRU recommendations are taken from Ref. [12].

projectile-electron has the same velocity as the incoming ion and the electron cross sections are taken from Ref. [3]) . Calculated He^{2+} ionization cross sections agree well with experimental data for water vapor [7, 11] for larger incident ion energies. The bare Z_0^2 scaling clearly overestimates non-PWBA corrections at lower energies, as mentioned earlier. Calculated He^{+} ionization cross sections agree in magnitude and follow the general trend of experimental data for water vapor [10, 11]. No experimental data for He^{0} impact are available.

Excitation cross sections have been calculated using the semiempirical model for proton impact described in Ref. [4] and the same effective charge scaling were applied as for ionization. Stopping cross sections σ_{st} are calculated and displayed in the right panel of Fig. 1 together with contributions from the different charge states ($\Phi_i\sigma_{\mathrm{st},i}$ and charge changing events $\sigma_{\mathrm{st,ct}}$. Charge changing cross sections as well as calculation of the

stopping cross sections are described and discussed in the following sections. The total stopping cross section agrees well with ICRU recommendations [12] at higher incident ion energies, while at lower ion energies contributions from He^+ and He^0 are clearly underestimated.

The model introduced by McGuire et al. [13] is based on a plane-wave Born approximation using hydrogenic wave functions. The projectile-electron–target-electron interaction is considered in an implicit and semiempirical way. Simple analytic expressions for the effective charge of a projectile carrying 0, 1, or 2 hydrogenic electrons are derived within this model and given by

$$\mathrm{He}^{2+} \quad : \quad Z_{\mathrm{eff}}^2 = Z_0^2 \tag{10}$$

$$\mathrm{He}^{+} \quad : \quad Z_{\mathrm{eff}}^2 = Z_0^2 + 1 - 2Z_0 \left(\frac{4\hat{R}^2}{4\hat{R}^2 + 1} \right)^2 \tag{11}$$

$$\mathrm{He}^{0} \quad : \quad Z_{\mathrm{eff}}^2 = Z_0^2 + 2 - 4Z_0 \left(\frac{4\hat{R}^2}{4\hat{R}^2 + 1} \right)^2 + 2 \left(\frac{4\hat{R}^2}{4\hat{R}^2 + 1} \right)^4 . \tag{12}$$

Here, $\hat{R}$ is the same scaled adiabatic interaction radius as given above. Note, that electron–electron interactions are considered implicitly. This leads to the fact that the effective charge Z_{eff}^2 for He^+ impact goes to $(Z_0 - 1)^2$ for large interaction distances, as expected, and to $Z_0^2 + 1 > Z_0^2$ for very small interaction distances.

Ionization and stopping cross sections calculated within this model are shown in Fig. 2. For the calculations, an effective Slater charge of Q_{eff} = 1.7 was used for He^+ and Q_{eff} = 1.4 for He^0 (2 electrons in the $1s$ shell). Again, total ionization cross sections are in reasonable agreement with experimental data. Total ionization cross sections for He^{2+} impact remain the same compared to model 1 (the same Z_0^2 scaling), values for He^+ and He^0 impact are slightly larger in this model. This changes the contributions to the stopping cross sections, as seen on the right panel of Fig. 2. Again, at high incident energies the total stopping cross section agree well with ICRU recommendations. At intermediate incident energies the agreement seems better than in Toburen's model, but the stopping cross section still underestimates recommendations. At small incident energies the contributions of He^0 are larger than the ICRU recommendations.

McGuire and co-workers [13] also compare their analytically calculated effective charges with that ones obtained by the above mentioned model by Toburen and co-workers [8] and with experimental data. They find that both model calculations predict effective charges shifted to somehow smaller interaction distances compared to experimental data (Fig. 2 and 3 of Ref. [13]), but describe the distance dependency fairly well. Model calculations are based on the fact that the electrons which shield the nuclear charge are in the atomic $1s$ subshell, i.e., the projectile in its ground state. One possibility to account for somehow larger interaction distances with similar effective charges is to allow the projectile to be in excited states. Charge distributions in "higher" orbits extent to larger radii, which leads to increased interaction distances compared to the ground state. And strictly speaking, there is a high probability that the projectile may get excited or even ionized in collisions [14].

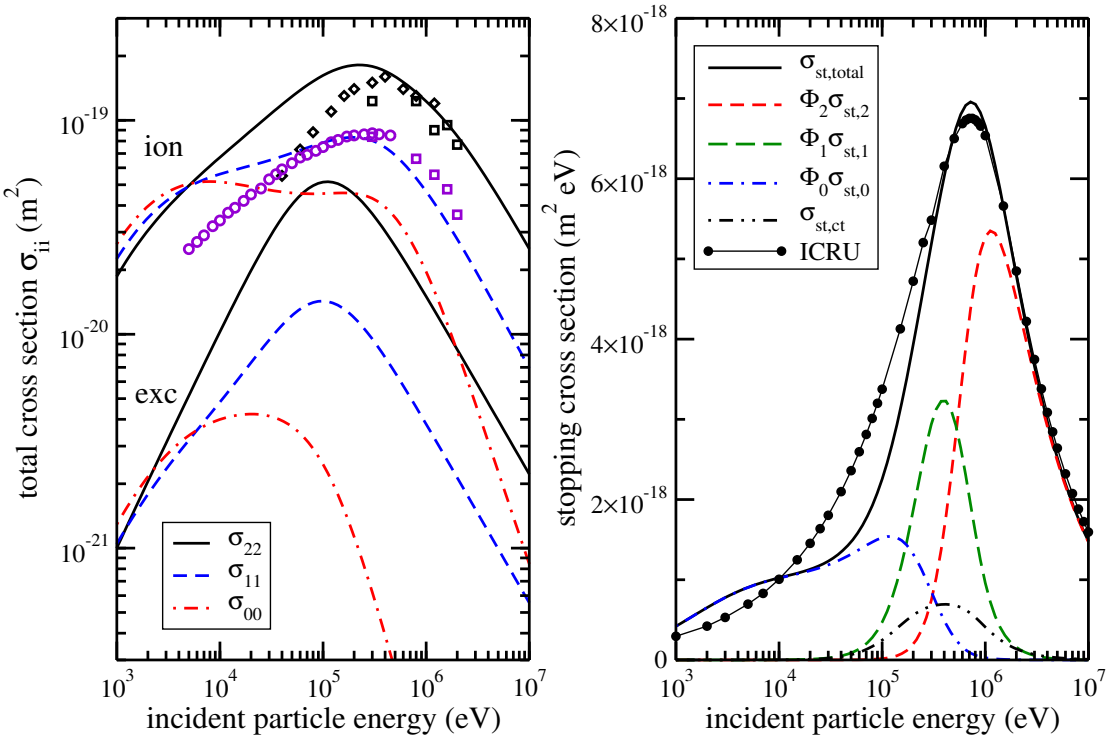

Figure 2: Ionization and stopping cross sections for helium impact on liquid water using the effective charge model of McGuire et al. [13]. The left panel shows total ionization (ion) and excitation (exc) cross sections for the different charge states ($i = 0, 1, 2$) together with experimental data for ionization taken from Refs. [7] (diamonds), [10] (circles), and [11] (squares). The right panel illustrates contributions to the total stopping cross sections from the different charge states ($\Phi_i\sigma_{\mathrm{st},i}, i = 0, 1, 2$) and charge changing processes ($\sigma_{\mathrm{st,ct}}$). The ICRU recommendations are taken from Ref. [12].

Taking advantage of what we learned from the two models presented we adopt our final model for representing effective charges. This model is based again on the model of Toburen et al. [8], but considers explicitely simultaneous projectile excitation (projectile ionization is included in the modeling of the charge changing cross sections). When calculating the screening function $S(R)$, we allow the projectile electrons to be in the $1s$, $2s$ or $2p$ state. In detail, for He^+ we consider the bound electron to be in the ground state 70 percent of the time and in the $n = 2$ level 30 percent of the time (15 percent each for the $2s$ and $2p$ state). For He^0 we consider the two electrons to be in the ground state 50 percent of the time and in the $n = 2$ excited state also 50 percent of the time (again 25 percent each for the $2s$ and $2p$ state, respectively). The effective charge Z_{eff} in our model is given by Eq. (6) using the following screening functions:

$$\mathrm{He}^{2+} \quad : \quad S(R) = 0, \tag{13}$$

$$\mathrm{He}^{+} \quad : \quad S(R) = 0.70 \cdot S(R)_{1s} + 0.15 \cdot S(R)_{2s} + 0.15 \cdot S(R)_{2p}, \tag{14}$$

$$\mathrm{He}^{0} \quad : \quad S(R) = 0.50 \cdot S(R)_{1s} + 0.25 \cdot S(R)_{2s} + 0.25 \cdot S(R)_{2p}. \tag{15}$$

Effective Slater charges of Q_{eff} = 2.0 are used for one electron in the $1s$ shell, Q_{eff} = 1.7 for two electrons in the $1s$ shell and Q_{eff} = 1.15 for one electron in the $2s$ or $2p$ shell, respectively. Additionally, projectile-electron – target electron interactions are considered as described earlier when using Toburen's model.

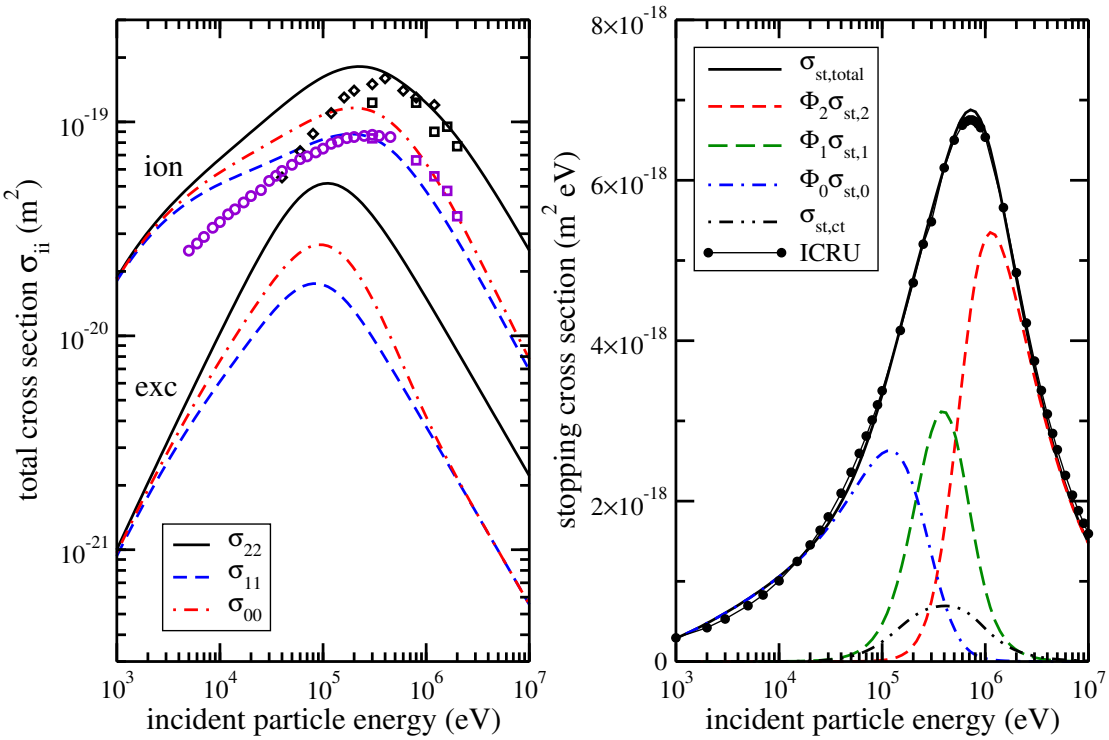

Figure 3: Ionization and stopping cross sections for helium impact on liquid water using our effective charge model. The left panel shows total ionization (ion) and excitation (exc) cross sections for the different charge states ($i = 0, 1, 2$) together with experimental data for ionization taken from Refs. [7] (diamonds), [10] (circles), and [11] (squares). The right panel illustrates contributions to the total stopping cross sections from the different charge states ($\Phi_i \sigma_{\mathrm{st},i}$, $i = 0, 1, 2$) and charge changing processes ($\sigma_{\mathrm{st},ct}$). The ICRU recommendations are taken from Ref. [12].

Figure 3 displays total ionization and stopping cross sections obtained with this model. Total ionization cross sections are in reasonable agreement with experimental data. Total cross sections for ionization and excitation by He^{0} impact are significantly larger compared to the two other models. They are even larger than total ionization cross sections for He^{+} impact. This fact agrees with the trend seen in electron production

cross sections in collisions of helium ions incident on helium, as reported in the book by McDaniel et al. (Fig. 4-2-7 of Ref. [15]). With the enhanced ionization cross sections for He^0 calculated stopping cross sections now agree very well with the ICRU recommended values over the whole incident energy range.

5 CHARGE CHANGING EVENTS

Charge changing cross sections σ_{ij} (change from charge state i to charge state j) are described in a semiempirical model, discussed in detail in Ref. [4]. The cross section is represented by

$$\sigma_{ij} = 10^{Y(X)}, \quad \text{with} \quad X = \log \tau, \tag{16}$$

where τ is the incident ion energy in eV, and

$$Y(X) = \left[a_0 X + b_0 - c_0 (X - x_0)^{d_0} \Theta(X - x_0)\right] \Theta(x_1 - X) + (a_1 X + b_1)\Theta(X - x_1), \tag{17}$$

with

$$x_1 = \left(\frac{a_0 - a_1}{c_0 d_0}\right)^{1/(d_0 - 1)} + x_0, \quad b_1 = (a_0 - a_1)x_1 + b_0 - c_0 (x_1 - x_0)^{d_0}. \tag{18}$$

Parameters are obtained by "fitting" σ_{ij} to rarely existing experimental data. It is assumed that similar cross sections (i.e. σ_{01} and σ_{02}) behave asymptotically in a similar way and that both, the liquid and the gas phase show similar behaved cross sections. Parameters used in calculations for the stopping cross sections in Figs. 1 – 3 are displayed in Table I.

Table I: Parameters used in the semiempirical formulas for charge changing cross sections σ_{ij}.

	σ_{01}	σ_{02}	σ_{12}	σ_{21}	σ_{20}	σ_{10}
a_0	2.25	2.25	2.25	0.95	0.95	0.65
b_0	-30.93	-32.61	-32.10	-23.00	-23.73	-21.81
a_1	-0.75	-0.75	-0.75	-2.75	-2.75	-2.75
c_0	0.590	0.435	0.600	0.215	0.250	0.232
d_0	2.35	2.70	2.40	2.95	3.55	2.95
x_0	4.29	4.45	4.60	3.50	3.72	3.53

Experimental data on charge changing cross sections for alpha particle impact on H_2O are rare and limited in energy range. No direct measurement of neutral He impact on H_2O is known. Data used for determining the parameters for neutral He impact are obtained from collisions with other molecules [16] using Bragg additivity rules, data obtained for He^{2+} and He^{+} impact are taken from Refs. [7, 10, 17].

6 STOPPING CROSS SECTIONS

Within the charge state approach [18], the total stopping cross section $\sigma_{\rm st}$ is given by

$$\sigma_{\rm st} = \sum_{i,j,i\neq j} \Phi_i(\sigma_{{\rm st},i} + \sigma_{ij}T_{ij}), \qquad \sigma_{{\rm st},i} = \int E\frac{{\rm d}\sigma_{ii}}{{\rm d}E}\,{\rm d}E, \tag{19}$$

where Φ_i are the probabilities to find the ion in charge state i, $\sigma_{{\rm st},i}$ the stopping cross section for the charge state i, and σ_{ij} the cross section for changing from charge state i to charge state j with energy transfer T_{ij}. Experimental and other theoretical information on the total stopping cross section is also used to guide and adjust parameters for the semiempirical models.

It is clear from Eq. 19 that all ionization cross sections of the different charge states as well as all charge changing cross sections contribute to the total stopping cross section. The total stopping cross sections as calculated with the different models for effective charges are displayed in Figs. 1 - 3, respectively.

7 CONCLUSIONS

In this work we have reviewed and presented different models for effective charge scaling of ionization cross sections for dressed ion (helium) impact on liquid water. As benchmark we have calculated the stopping cross sections and compared them to ICRU recommendations. We adopted and modified the model from Toburen et al. and adjusted the parameters from semiempirical formulas in such a way that the stopping cross section was best reproduced. Within this model it was necessary to consider also projectile excitation (and ionization) in order to reproduce the recommended stopping cross sections. The derived interaction cross sections have been implemented in the biophysical Monte Carlo simulation code PARTRAC, which can be used for event-by-event simulations in radiation biology [19].

8 ACKNOWLEDGMENTS

This work has been partially supported by the European Community (Contract No. FIGH-CT-1999-0005), by a Marie-Curie Individual fellowship (FIGD-CT-1999-50002), the Low Dose Radiation Research Program (BER), U.S. DoE (Grant no. DE-FG02-01ER63233) and by the NASA Office of Biological and Physical Research (OBPR)(Grant no. NNJ04HF39G).

9 REFERENCES

1. U. Fano, "Penetration of protons, alpha particles and mesons," *Ann. Rev. Nucl. Sci.*, **13**, pp 1–66.
2. S. Segui, M. Dingfelder, J.M. Fernández-Varea, and F. Salvat, "The structure of the Bethe ridge. Relativistic Born and impulse approximations," *J. Phys. B: At. Mol. Opt. Phys.*, **35**, pp. 33-53 (2002).

3. M. Dingfelder, D. Hantke, M. Inokuti, and H.G. Paretzke, "Electron inelastic-scattering cross sections in liquid water," *Radiat. Phys. Chem.*, **53** pp. 1-18 (1998).
4. M. Dingfelder, M. Inokuti, and H.G. Paretzke, "Inelastic-collision cross sections of liquid water for interactions of energetic protons," *Radiat. Phys. Chem.*, **59**, pp. 255–275 (2000).
5. J.M. Fernández-Varea, F. Salvat, M. Dingfelder, and D. Liljequist, "A relativistic optical-data model for inelastic scattering of electrons and positrons in condensed matter," *Nucl. Instr. Meth B.*, accepted for publication (2004).
6. M.E. Rudd, Y.-K. Kim, D.H. Madison, and T.J. Gay, "Electron production in proton collisions with atoms and molecules: energy distribution," *Rev. Mod. Phys.*, **64**, pp. 441–490 (1992).
7. M.E. Rudd, T.V. Goffe, and A. Itoh, "Ionization cross sections for 10-300 keV/u and electron-capture cross sections for 5-150 keV/u $^{3}He^{2+}$ ions in gases," *Phys. Rev. A,* **32**, pp. 2128–2133 (1985).
8. L.H. Toburen, N. Stolterfoht, P. Ziem, and D. Schneider, "Electronic screening in heavy-ion – atom collisions," *Phys. Rev. A*, **24** pp. 1741–1745 (1981).
9. J.C. Slater, "Atomic shielding constants," *Phys. Rev.*, **36** pp. 57–64 (1930).
10. M.E. Rudd, A. Itoh, and T.V. Goffe, "Cross sections for ionization, capture, and loss for 5-450 keV He^{+} on water vapor," *Phys. Rev. A*, **32** pp. 2499–2500 (1985).
11. L.H. Toburen, W.E. Wilson, and R.J. Popowich, "Secondary electron emission from ionization of water vapor by 0.3 to 2.0 MeV He^{+} and He^{2+} ions," *Radiat. Res.*, **82** pp. 27–44 (1980).
12. International Commission on Radiation Units and Measurements, *Stopping powers and ranges for protons and alpha particles*, ICRU Report 49, ICRU, Bethesda, MD, U.S.A. (1993).
13. J.H McGuire, N. Stolterfoht, and P.R. Simony, "Screening and antiscreening by projectile electrons in high-velocity atomic collisions," *Phys. Rev. A*, **24** pp. 97–102 (1981).
14. S.T. Manson and L.H. Toburen, "Energy and angular distributions of electrons from fast He^{+} + He Collisions," *Phys. Rev. Lett.*, **46**, pp. 529–531 (1981).
15. E.W. McDaniel, J.B.A. Mitchell, and M.E. Rudd, *Atomic collisions: Heavy particle projectiles*, John Wiley and Sons, New York, NY, U.S.A. (1993).
16. M. Sataka, A. Yagishita, and Y. Nakai, "Measurement of charge-changing cross sections in collisions of He and He^{+} with H_2, O_2, CH_4, CO and CO_2," *J. Phys. B. At. Mol. Opt. Phys.*, **23**, pp. 1225-1234 (1990).
17. M.E. Rudd, T.V. Goffe, A. Itoh, and R.D. DuBois, "Cross sections for ionization of gases by 10-2000 keV He^{+} ions and for electron capture and loss by 5-350 keV He^{+} ions," *Phys. Rev. A*, **32** pp. 829–835 (1985).
18. S.K. Allison and S.D. Warshaw, "Passage of heavy particles through matter," *Rev. Mod. Phys.*, **25**, pp. 779–817 (1953).

19. W. Friedland, M. Dingfelder, P. Jacob, and H.G. Paretzke, "Calculated DNA double-strand break and fragmentation yields after irradiation with He ions," *Radiat. Phys. Chem.*, **72**, pp. 279–286 (2005).